Lab on a Chip

Cite this: *Lab Chip*, 2012, **12**, 4986–4991

www.rsc.org/loc

PAPER

Large-scale femtoliter droplet array for digital counting of single biomolecules†

Soo Hyeon Kim,[ab] Shino Iwai,[bc] Suguru Araki,[bc] Shouichi Sakakihara,[c] Ryota Iino[ab] and Hiroyuki Noji*[ab]

Received 1st June 2012, Accepted 14th August 2012
DOI: 10.1039/c2lc40632b

We present a novel device employing one million femtoliter droplets immobilized on a substrate for the quantitative detection of extremely low concentrations of biomolecules in a sample. Surface-modified polystyrene beads carrying either zero or a single biomolecule-reporter enzyme complex are efficiently isolated into femtoliter droplets formed on hydrophilic-in-hydrophobic surfaces. Using a conventional micropipette, this is achieved by sequential injection first with an aqueous solution containing beads, and then with fluorinated oil. The concentration of target biomolecules is estimated from the ratio of the number of signal-emitting droplets to the total number of trapped beads (digital counting). The performance of our digital counting device was demonstrated by detecting a streptavidin-β-galactosidase conjugate with a limit of detection (LOD) of 10 zM. The sensitivity of our device was >20-fold higher than that noted in previous studies where a smaller number of reactors (fifty thousand reactors) were used. Such a low LOD was achieved because of the large number of droplets in an array, allowing simultaneous examination of a large number of beads. When combined with bead-based enzyme-linked immunosorbent assay (digital ELISA), the LOD for the detection of prostate specific antigen reached 2 aM. This value, again, was improved over that noted in a previous study, because of the decreased coefficient of variance of the background measurement determined by the Poisson noise. Our digital counting device using one million droplets has great potential as a highly sensitive, portable immunoassay device that could be used to diagnose diseases.

Introduction

Biomolecules, especially protein biomarkers, are widely used for the clinical diagnosis of diseases. The capacity to detect small numbers of biomolecules at low concentrations is critical for the early diagnosis of diseases, which, in turn, indicates the treatment regimens to be followed.[1] Enzyme-linked immunosorbent assay (ELISA) is widely used for the detection of protein biomarkers, as it amplifies the signals by using enzymes conjugated with antibodies. The conventional ELISA has a limit of detection (LOD) of about 1 pM concentration of the target,[2] where the ensemble of enzymes are measured in a relatively large reactor volume (μL). An effective strategy for high-sensitivity detection using ELISA is to isolate each biomolecule-enzyme complex into ultra-small reactor volumes, one at a time. Since the reaction products generated from single enzymes accumulate inside femtoliter reactors, detection of a single biomolecule-enzyme complex with a conventional fluorescence microscope is rendered possible.[3,4]

For high-throughput, simultaneous and parallel analyses of single biomolecule–enzyme complexes, many femtoliter reactors within each array are required. Continual advances in microfabrication technology have facilitated the creation of such arrays with single-molecule detection ability. In previous studies, we proposed a simple method for preparing a femtoliter microchamber array by pressing a polydimethylsiloxane (PDMS) sheet against a cover glass to enclose microwell structures fabricated on the surface of PDMS.[3,5–7] The PDMS femtoliter microchamber array was used for the single-molecule enzymatic assay of β-galactosidase and horseradish peroxidase enclosed in the chamber with fluorogenic substrates[3,4,8] and for the estimation of the chemomechanical coupling efficiency of a rotary motor protein F_1-ATPase.[9,10] This concept was then extended to the development of another type of microchamber consisting of a prefabricated fiber optic bundle, which has microcavities on the tip and silicone sheets to seal microcavities.[4,11] Alternatively, PDMS microwells can be combined with elastomeric membranes.[8] However, all these approaches require mechanical micromanipulation to enclose the microchamber array tightly, which, in turn, requires precise control and proficient skills. These drawbacks could be eliminated with the use of water-in-oil droplets. Microfluidics approaches for droplet

[a]*Department of Applied Chemistry, Graduate School of Engineering, The University of Tokyo, Hongo 7-3-1, Bunkyo-ku, Tokyo 113-8656, Japan. E-mail: iino@appchem.t.u-tokyo.ac.jp; hnoji@appchem.t.u-tokyo.ac.jp*
[b]*CREST, Japan Science and Technology Agency, Sanbancho 5, Chiyoda-ku, Tokyo 102-0075, Japan*
[c]*Institute of Scientific and Industrial Research, Osaka University, Mihogaoka, 8-1, Ibaraki, Osaka, 567-0047, Japan*
† Electronic supplementary information (ESI) available: See DOI: 10.1039/c2lc40632b

generation were successfully applied for high-throughput PCR amplification of single DNA template molecules.[12] However, for the high-sensitivity detection of single-molecule enzymatic activities, the droplets have to be small (down to femtoliter level) to concentrate the small number of reaction products, and immobilized on a substrate to gain sufficiently long observation time. Recently, we reported a more advanced method for preparing a femtoliter droplet array on a hydrophilic-in-hydrophobic micropatterned surface *via* the sequential injection of aqueous solution and oil. This method was successfully used to measure the kinetic parameters of a single β-galactosidase and a single F_1-ATPase enclosed in a droplet.[13]

In addition to facilitating single-molecule enzymatic assays, arrayed microchambers allow high-sensitivity detection of target biomolecules. By separating individual molecules into the arrayed reactors, each reactor can be categorized into a binary scale – "1" for a reactor containing a single biomolecule or a "0" if no biomolecule is present. The concentration of target biomolecules is estimated by counting the number of positive reactors (digital counting). The concept of "digital counting" was first applied to digital PCR for the quantification of nucleic acids by partitioning a sample followed by PCR amplification.[14,15] Recently, Duffy and coworkers employed this concept to count the number of protein biomolecules with digital ELISA. The femtoliter microchambers, formed by pressing etched optical fiber against a silicone gasket, were used to isolate single biomolecule–enzyme complexes captured on paramagnetic beads.[16] They successfully demonstrated high-sensitivity detection of streptavidin-β-galactosidase conjugate (SβG) by streptavidin-biotin interaction and a clinical biomarker prostate-specific antigen (PSA), where the LODs were 220 zM and 50 aM, respectively.

Although the above study is an impressive proof-of-concept, many aspects of the digital counting approach can be further optimized. First, since the single biomolecule–enzyme complex is captured on a bead, the inherent LOD of the digital counting is determined by the bead throughput capability of the device. In other words, increasing the number of beads examined will improve the LOD. To examine a large number of beads simultaneously, the number of femtoliter reactors should be increased to effectively isolate beads. Moreover, counting a large number of signal-emitting reactors decreases the coefficient of variance (CV) of measurement, since the imprecision of digital counting is mainly determined by the Poisson noise of counting.[16] Second, improvements over previous devices are required to circumvent the complexities of the high centrifugal force needed for bead trapping and the skilful micromanipulation of optical fiber arrays needed for chamber sealing.

Here, we propose a novel device utilizing one million femtoliter droplets in an array to achieve high-sensitivity detection of protein biomarkers with digital counting. Fig. 1a shows the concept of the approach. The single target biomarker bound with an enzymatic reporter is captured on a polystyrene bead having a functionalized surface. When the ratio of beads to biomarker–reporter complexes is 10 : 1, 99% of beads carry either single complexes or none, according to the Poisson distribution. Each bead is isolated within the femtoliter droplet array immobilized on a substrate. Fluorescent products generated by the reporter enzymes accumulate within femtoliter

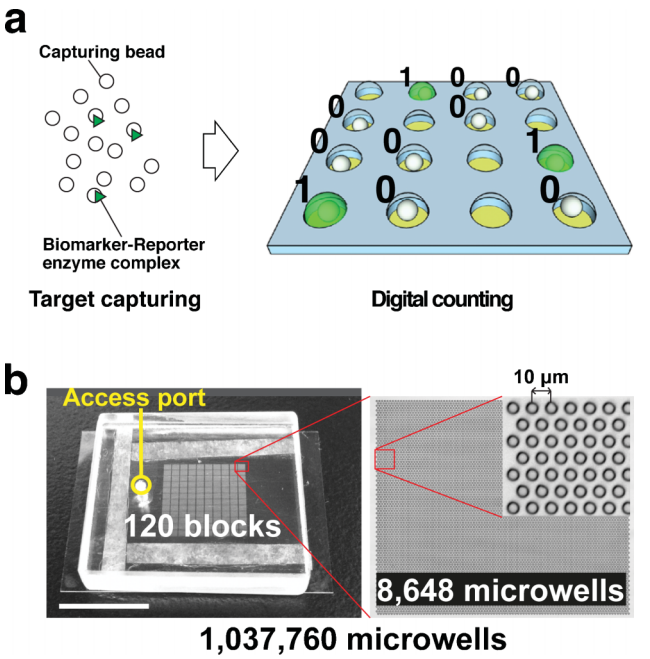

Fig. 1 Digital counting device. (a) Schematic illustrations of the concept of digital counting. Single biomolecule–reporter enzyme complexes are statistically captured on the surface-modified polystyrene beads. Single beads are isolated into femtoliter droplet array with the fluorogenic substrate of reporter enzyme. Each droplet, which contains a bead, is categorized in a binary scale with "1" being signal-emitting droplets and "0" the droplets without signal based on the fluorescence. Counting the number of "1" and "0" droplets allows estimation of the ratio of biomolecules to the beads. (b) Fabricated device, where the substrate of large array of hydrophilic-in-hydrophobic structures is assembled with CYTOP-coated glass that has an access port for sample injection. An array of CYTOP through-hole structure (5 μm in diameter, 3 μm in thickness, 10 μm center-to-center distance) is fabricated on a glass substrate. There are 120 blocks of well array where each block has 8648 wells corresponding to the 10^6 microwells on a single substrate. Scale bar is 1 cm.

droplets. The small volume of the reactor allows direct observation of the fluorescent signal from a droplet containing a single reporter enzyme with a conventional optical microscope. The droplets, which contain a bead, are categorized into a binary scale – "1" for a signal-emitting droplet or "0" for droplets without signals. The concentration of target biomolecules in a sample is estimated by counting the number of signal-emitting droplets together with the number of trapped beads. To achieve this, a highly efficient bead-trapping function was integrated into our previous platform of surface-immobilized droplet arrays formed on a hydrophilic-in-hydrophobic micropatterned surface.[13] Our novel device allows formation of femtoliter water-in-oil (W/O) droplet array and concomitant isolation of single beads into droplets by sequential injection of aqueous solution with suspended beads and fluorinated oil with a conventional micropipette. Our study complements and further advances the approaches performed by Duffy and collaborators[16,17] and Walt and collaborators,[18] in the sense that a large number of droplet arrays are used to improve sensitivity of the digital counting device. Since one million droplets allowed us to simultaneously examine 7×10^5 beads for the presence of biomolecules, we

achieved a LOD of 10 zM for the detection of SβG. Moreover, digital ELISA of PSA showed a LOD of 2 aM, which was improved 25-fold compared with previous studies. Such an improvement on the digital ELISA was achieved by decreasing the Poisson noise attributed to counting beads without target (background), by using the large number of droplets in an array.

Experimental

Fabrication of the device

To immobilize W/O droplets on the surface of the device, we fabricated hydrophobic through-hole structures on a hydrophilic glass substrate. A hydrophobic polymer of carbon–fluorine (CYTOP, Asahi-glass, Japan) was spin-coated on a clean coverglass (Matsunami, Japan) at 2000 rpm for 30 s, and then baked for 1 h at 180 °C. This process was repeated 4 times for the appropriate thickness of the CYTOP layer, *i.e.*, 3 μm, whose thickness is comparable with the diameter of polystyrene beads. Photolithography was carried out with a positive photoresist (AZP4903, AZ Electronic Materials, Japan) to pattern mask structure on the CYTOP layer. The resist-patterned substrate was dry-etched with O_2 plasma by a reactive ion etching system (RIE-10NR, Samco, Japan) to expose an array of hydrophilic SiO_2 glass surface. The substrate was then cleaned and rinsed with acetone and ethanol to remove the photoresist layer remaining on the substrate. Since the fabrication process was well established, we were able to efficiently fabricate hydrophobic through-hole structures on a hydrophilic glass substrate, where the fabrication success rate was 100%, as well as the success rate of using the device. To increase surface-to-volume ratio, a flow cell was formed by assembling CYTOP coated glass, which has an access port for sample injection, on the microwell array with a spacer. Fig. 1b shows a fabricated device, where the diameter of the CYTOP well is 5 μm, which is slightly bigger than that of the target beads (3 μm) for efficient trapping, and the center-to-center distance is 10 μm. There are 120 blocks of well arrays, where each block has 8648 wells corresponding to 10^6 CYTOP wells on a single substrate in total.

Reagents

For the detection of the streptavidin–biotin interaction, amino-modified polystyrene beads (3 μm in diameter, Micromod, Germany) were biotinylated using a biotinylation reagent, NHS-PEG4-Biotin (Thermo scientific, USA). Streptavidin-β-galactosidase (SβG) and its fluorogenic substrate, fluorescein di-β-D-galactopyranoside (FDG), were purchased from Invitrogen (USA). For the ELISA of prostate specific antigen (PSA), purified PSA molecules and monoclonal anti-PSA antibodies for sandwich ELISA were purchased from BiosPacific (USA). To prepare capture antibody-coated beads, the biotinylation reagent NHS-PEG4-Biotin was reacted with amino groups of capture antibodies. The biotinylated capture antibodies were conjugated with streptavidin beads that were prepared from a reaction of the biotinylated beads and streptavidin (Type II, Wako, Japan). About 10^5 capture antibodies were coated on a single polystyrene bead. For the preparation of detection antibody-β-galactosidase conjugate, β-galactosidase (Roche, Japan) was conjugated with the detection antibody by using the reagent MAL-PEG-SCM-3400 (Laysan Bio Inc., USA), where a maleimide group of the reagent was reacted with a thiol group of the β-galactosidase, and a SCM ester of the reagent was reacted with an amino group of the detection antibodies.

Droplet formation and bead enclosure

Beads suspended in aqueous solution were injected into the access port with a micropipette (Gilson, USA).[19] Since the microwell structure was fabricated with hydrophobic materials, the aqueous solution did not fill the microwells, and air, therefore, remained inside the microwells. To remove this air, the device was placed into a vacuum chamber (As One, Japan) to apply negative pressure for 1 min. Then, the beads were settled by gravity for several minutes and trapped into the microwells by injecting fluorinated oil (Fluorinert FC40, Sigma, USA). High-density (1.85 g mL^{-1}) oil allowed efficient removal of the aqueous solution from the hydrophobic CYTOP surface. On the other hand, the hydrophilic SiO_2 surfaces at the bottom of the microwells retained the aqueous solution with trapped beads. Since the beads went out from the device without trapping with fast injection rate of oil, we slowly injected oil (< 40 μL s^{-1}) by using micropipette (200 μL) for efficient beads trapping.

Digital counting of SβG

Biotinylated beads (3×10^6 particles) were mixed with various concentrations of SβG from 0.01 to 1000 aM in a test tube. After reaction for 30 min at room temperature, the beads were washed and injected into the device with the fluorogenic substrate of β-galactosidase, namely, FDG (2.5 mM). The beads were settled for 10 min, and trapped into the droplet array by injecting fluorinated oil. The oil used is biocompatible with β-galactosidase and efficiently isolates the fluorescent product, *i.e.*, fluorescein, which allows a single-molecule enzymatic assay of β-galactosidase.[13] The device was incubated at room temperature for up to 5 h to increase the signal-to-noise ratio.

Digital ELISA of PSA

Various concentrations of PSA molecules were reacted with the capturing beads (8×10^6 particles) and detection antibodies (4 pM) in a test tube (100 mM phosphate buffer, pH 7.4, 0.5% BSA) for 2 h at room temperature. After the reaction, the beads were washed 5 times to remove unbounded detection antibodies, and then mixed with the fluorogenic substrate FDG (2.5 mM). For the detection of PSA with digital ELISA, the beads were introduced into the digital counting device and trapped into the droplets in an array after the settlement of beads for 5 min. For comparison, bead-based conventional sandwich ELISA was also carried out. The signal from the ensemble of beads was recorded with a fluorescence plate reader. The slope of the fluorescence signal increase with time was measured for each concentration of PSA ([PSA]).

Image acquisition and data analysis

For obtaining bright-field and fluorescence images of droplet array, the device was mounted on the motorized *x*–*y* translational stage located on a focus drift compensating microscope (IX81-ZDC2, Olympus, Japan) for continuous autofocusing.

The images were acquired with a Scientific CMOS camera (Neo sCMOS camera, Andor Technology Plc, USA). The stage and the camera were controlled by commercial software (MetaMorph, Molecular devices, USA). Bright-field and fluorescence images of one droplet array block were acquired sequentially. Then, the stage was moved to acquire images of the next block in an array. With this setup, bright-field and fluorescence images for one million droplets in an array were acquired in 8 min. From the obtained images, the fraction of bright droplets was determined by the following equation: $N_{bD}/N_{tB} \times 100\%$, where N_{bD} and N_{tB} are the number of bright droplets and trapped beads, respectively.

Results and discussion

Bead-trapping efficiency

The large number of hydrophilic surfaces at the bottom of a hydrophobic microwell structure is designed for the efficient isolation of each bead into the femtoliter droplets. Fig. 2a shows a schematic illustration of the bead-trapping process. First, aqueous solution with the beads is injected into an access port with a conventional micropipette. Injected beads are settled on the surface of the microwell array, because of gravity, for several minutes. Then, the beads are swept into microwells with an advancing W/O interface induced by injection of oil through the access port with the micropipette. Since the microwell has a hydrophilic surface at the bottom of a hydrophobic well structure, aqueous solution with a single bead is immobilized on the bottom of the well, while hydrophobic surfaces are covered with oil (Fig. 2b). The simple device allows the formation of one million femtoliter droplets with beads in parallel in several minutes by the sequential injection of aqueous solution and oil, without the need for complex equipment associated with fluidic control (Video S1, ESI†). Moreover, a larger number of droplets can be prepared by increasing the density of the well and increasing the number of blocks of well array on a substrate (see Fig. 1b). By increasing the scale of the array, we can further increase the bead throughput capability. This would be practically difficult for the microfluidic approaches generating droplets in serial, which will take 1 h to prepare 3.6 million droplets even with the generation rate at kHz.

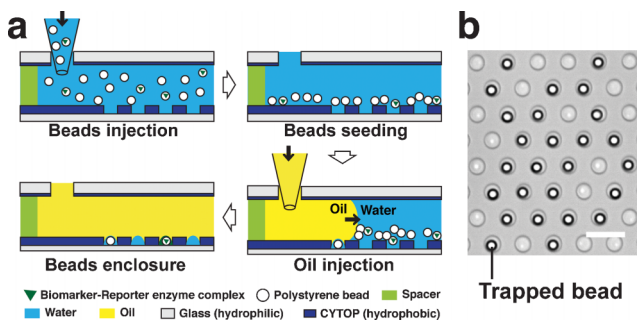

Fig. 2 Bead trapping. (a) Schematic illustrations of bead trapping. Aqueous solution with target beads is injected into the device through an access port by using a conventional micropipette. The injected beads are allowed to settle down, because of gravity, for several minutes. Then, oil is injected through the access port with a micropipette, where the W/O-interface sweeps the beads into the microwell. Since the bottom of the well is hydrophilic and the walls are hydrophobic, aqueous solution containing a single bead is immobilized on the bottom of the well, while the hydrophobic surfaces are covered with oil. (b) Three-micrometer polystyrene beads are trapped into the W/O droplets immobilized on the hydrophilic surface in the hydrophobic well structure. Around 60% of droplets are occupied by single beads. Scale bar is 10 μm.

For efficient bead trapping, we investigated the dependence of bead-trapping efficiency on the settlement time. About 3×10^6 beads were introduced into the device and allowed to settle for 5, 10, and 15 min. Then, we counted the number of trapped beads for each settlement time. The number of trapped beads gradually increased with the settlement time and reached a plateau at around 10 min, where 7×10^5 beads (23% of introduced beads) were trapped into the 10^6 droplet array (Fig. S1, ESI†). Another important parameter for efficient bead trapping was the number of introduced beads. Different numbers of beads were introduced into the device and trapped after settlement (5 or 10 min). The number of trapped beads was proportional to the number of introduced beads over a certain range (Fig. S2, ESI†). However, if very large numbers of beads were introduced, 2 or 3 beads became trapped within a single droplet. For instance, 34% of droplets contained 2 or 3 beads when 8×10^6 beads were introduced and allowed to settle for 10 min. These results illustrate that beads can be efficiently trapped by adjusting the number of introduced beads and controlling the settlement time.

The bead trapping efficiency can be further improved by optimizing the geometry of the microwells which changes the flow profiles inside the microwells. For instance, the triangular microwells, which showed good performance for single cell trapping,[20] would increase the beads trapping efficiency.

Inherent LOD of our digital counting device

To investigate the inherent LOD of our digital counting device, we demonstrated the detection of a conjugate between streptavidin and a reporter enzyme β-galactosidase, SβG, bound to the biotinylated beads by using the well-characterized streptavidin–biotin interaction. After enclosure of the bead into the droplet, we carried out time-lapse observation of the fluorescence signal from the droplets containing a bead bound with a single SβG molecule. Fig. 3 shows the representative fluorescence and bright-field images of a block of droplet array at the different concentrations of SβG in a sample (Video S2, ESI†). The number of bright droplets was proportionally decreased with the concentration of SβG ([SβG]). The fraction of bright droplets was proportionally changed with [SβG] over the 5 digits, indicating a wide dynamic range (Fig. 4a). Linear fitting of the data points at 0.01, 0.1, and 1 aM is shown in Fig. 4b. The LOD of SβG detection was determined from the extrapolation of [SβG] at a fraction of bright droplets equal to the background plus 3 times standard deviation (SD) of the background. The background was determined from the experiments without SβG molecules. Under these conditions, the LOD reached 10 zM, corresponding to 6 molecules mL^{-1}.

The inherent LOD, as well as the dynamic range of any digital counting device, is highly reliant on the number of reactors in an array. A large number of reactors in an array allows it to determine whether a small fraction of trapped beads are associated with reporter enzymes. The inherent LOD of our

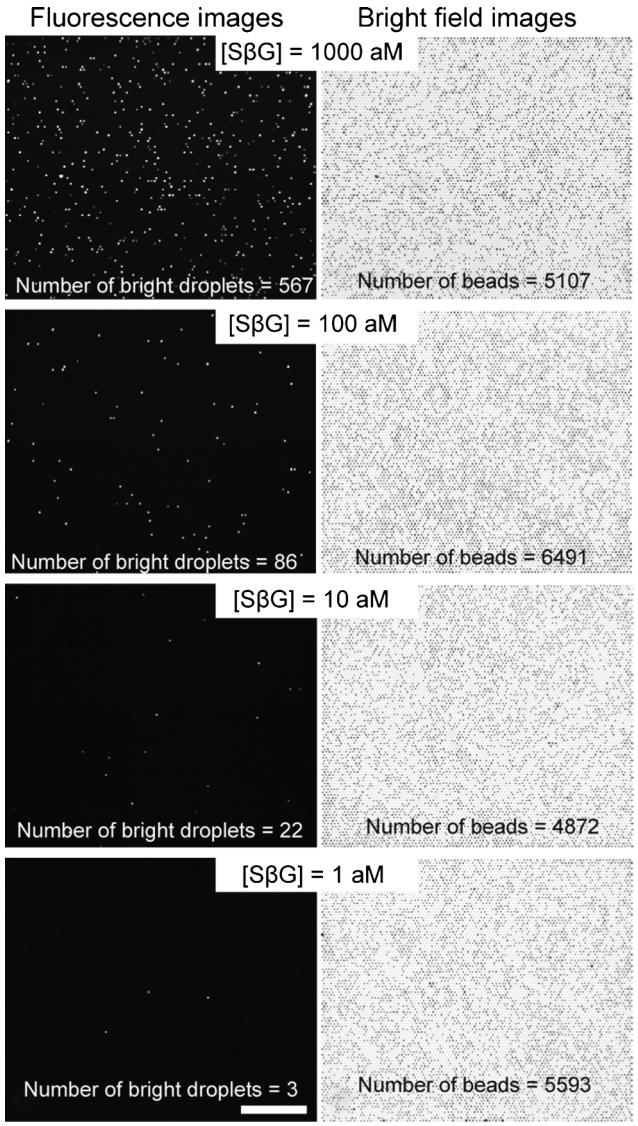

Fig. 3 Representative fluorescence (left column) and bright-field (right column) images of the droplet array for various concentrations of SβG molecules. The number of bright droplets proportionally decreased with the [SβG] in a sample, while the number of trapped beads did not change drastically. Scale bar is 200 μm.

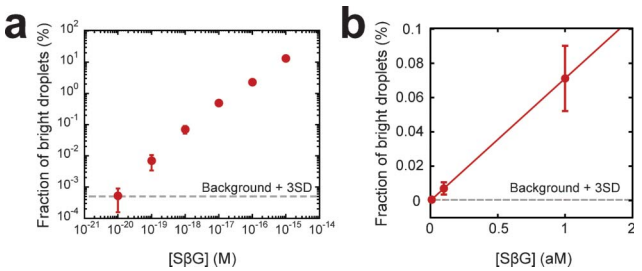

Fig. 4 Dependence of the fraction of signal-emitting droplets on [SβG]. [SβG] ranged from 10 zM to 1 fM, corresponding to 6 to 6 × 10^5 SβG molecules in the 1 mL solution. (a) Full plot shown in log–log scale. (b) Expanded plot with linear–linear scale. All data points include error bars that represent SD from three replicates. The limit of detection (LOD) was determined to be 10 zM.

device, 10 zM, is 22-fold improved compared to the results of Rissin *et al.*, (220 zM) utilizing 5 × 10^4 optical fiber microwells.[16] Statistically, 0.0004% of beads carry single-SβG molecules when 10 zM SβG molecules are reacted with 3 × 10^6 beads in a 1 mL solution. To detect such a low fraction of beads in an ensemble, at least 2.5 × 10^5 beads should be examined simultaneously, which requires sufficient number of droplets for the isolation of each bead. Since our device using one million droplets ensures simultaneous examination of 7 × 10^5 trapped beads, we have achieved a highly improved inherent LOD. Moreover, the ability for the examination of a large number of beads provides a wide dynamic range of detection in this system. The lower limit for the fraction of bright droplets is determined from the number of trapped beads when only a single droplet emits the signal. As a result, the inherent performance, LOD, as well as dynamic range, of the digital counting devices are determined by the number of reactors (droplets).

Application to digital ELISA

Our digital counting device was applied for the detection of the clinical biomarker PSA with bead-based ELISA. The LOD of PSA determined by conventional ELISA using a plate reader was 14 pM, obtained from the background plus 3 times the SD of the background, where the background was acquired without PSA molecules (Fig. S3, ESI†). In digital ELISA, the number of bright droplets in the fluorescence images, as well as the fraction of bright droplets, was proportional to the concentration of PSA (Fig. 5). The LOD of digital ELISA, determined as described above, was 2 aM. Our digital counting device showed 10^7-fold improvement in the LOD for ELISA of PSA compared with that of a plate reader.

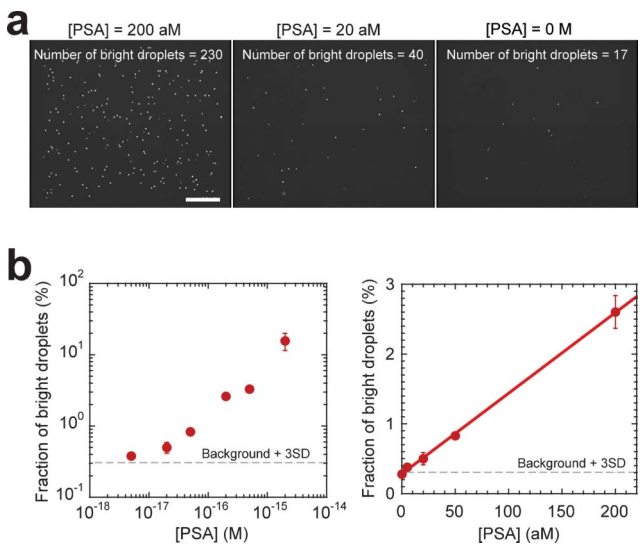

Fig. 5 Digital ELISA of PSA. (a) Representative fluorescence images of a block of droplet array for the various concentrations of PSA. Scale bar is 200 μm. (b) Dependence of the fraction of bright droplets on [PSA] shown in log–log scale (left) and linear–linear scale in the attomolar range (right). All data points include error bars that represent SD from three replicates. The limit of detection (LOD) was determined to be 2 aM.

Our demonstration showed >25-fold improved sensitivity for PSA detection compared to the previous reports on digital ELISA of PSA obtained by Rissin *et al.* (50 aM)[16] or Kan *et al.* (370 aM).[17] In our digital ELISA of PSA, 0.3% of droplets emitted a fluorescence signal even without PSA, due to the non-specific binding of the detection antibodies to the capturing beads. On the other hand, the SD of the background is basically determined by the Poisson noise. The CV of background in our measurement was 3%, comparable to the CV by the Poisson noise, *i.e.*, 2%, given by $1/\sqrt{n} \times 100\%$, where n is the average number of counted droplets. To further clarify the effect of number of droplets on the CV, we randomly selected one block (~8600 droplets) and 12 blocks (~100 000 droplets) of array, and calculated the background and CV for each case. The CV increased when we took less droplets into account, while the background did not change (Table S1, ESI†). Our background level (0.3%) of the fraction of bright droplets was only slightly better than those of previous studies, which might be caused by different experimental conditions. However, utilization of one million droplets allowed us to count 16 times more droplets, resulting in a 12-fold decrease in the CV of the background measurement, as compared to the results obtained by Rissin *et al.*[16] (Table S1, ESI†). These results indicate that increasing the number of droplets is an effective way to improve the LOD of digital ELISA, as it reduces the statistical error induced by Poisson noise.

Conclusions

In the digital counting, the number of reaction chambers sets the theoretical LOD. Therefore, it was expected that digital counting using a large number of chambers would improve the LOD. This point was demonstrated in the present work. Digital counting of SβG was carried out using our original microdevices employing one million droplets and its LOD was shown to reach 10 zM, which is 20 times lower than that of the previous work performed with fifty thousand reactors.[16] The large number of reactors also enhanced the dynamic range of detection (5 digits). Moreover, it was shown that a large number of reactors reduced the Poisson noise attributed to bead counting, resulting in improvement of LOD. In the digital ELISA of a clinical biomarker, PSA, one million droplets reduced the background noise and thus improved the LOD down to 2 aM (60 ag mL^{-1}), which is again >20 times lower than the reported value.[16] Thus, it was clearly proven that the large number of reaction chambers improves the LOD of digital counting by enhancing the detection sensitivity and reducing the Poisson noise of the background counting. Another advantageous feature of our method is that the present system does not require other equipment, such as a pump for sample injection or a micromanipulator for reactor sealing. This is critical when considering the integration with other micro-devices such as detection units for a highly sensitive point-of-care testing application. We suggest that our simple device fore-shadows the development of a highly integrated, portable Lab-on-a-chip device directly coupled with a CMOS image sensor.[21]

Acknowledgements

This research was supported by Japan Science and Technology Agency for Core Research for Evolutional Science and Technology (CREST).

References

1 P. R. Srinivas, B. S. Kramer and S. Srivastava, *Lancet Oncol.*, 2001, **2**, 698–704.
2 D. A. Giljohann and C. A. Mirkin, *Nature*, 2009, **462**, 461–464.
3 Y. Rondelez, G. Tresset, K. V. Tabata, H. Arata, H. Fujita, S. Takeuchi and H. Noji, *Nat. Biotechnol.*, 2005, **23**, 361–365.
4 D. M. Rissin and D. R. Walt, *Nano Lett.*, 2006, **6**, 520–523.
5 R. Iino, L. Lam, K. V. Tabata, Y. Rondelez and H. Noji, *Jpn J Appl Phys*, 2009, 48.
6 L. Lam, R. Iino, K. V. Tabata and H. Noji, *Anal. Bioanal. Chem.*, 2008, **391**, 2423–2432.
7 L. Lam, S. Sakakihara, K. Ishizuka, S. Takeuchi and H. Noji, *Lab Chip*, 2007, **7**, 1738–1745.
8 S. Y. Jung, Y. Liu and C. P. Collier, *Langmuir*, 2008, **24**, 4439–4442.
9 Y. Iko, K. V. Tabata, S. Sakakihara, T. Nakashima and H. Noji, *FEBS Lett.*, 2009, **583**, 3187–3191.
10 Y. Rondelez, G. Tresset, T. Nakashima, Y. Kato-Yamada, H. Fujita, S. Takeuchi and H. Noji, *Nature*, 2005, **433**, 773–777.
11 D. R. Walt, *Chem. Soc. Rev.*, 2010, **39**, 38–50.
12 B. J. Hindson, K. D. Ness, D. A. Masquelier, P. Belgrader, N. J. Heredia, A. J. Makarewicz, I. J. Bright, M. Y. Lucero, A. L. Hiddessen, T. C. Legler, T. K. Kitano, M. R. Hodel, J. F. Petersen, P. W. Wyatt, E. R. Steenblock, P. H. Shah, L. J. Bousse, C. B. Troup, J. C. Mellen, D. K. Wittmann, N. G. Erndt, T. H. Cauley, R. T. Koehler, A. P. So, S. Dube, K. A. Rose, L. Montesclaros, S. Wang, D. P. Stumbo, S. P. Hodges, S. Romine, F. P. Milanovich, H. E. White, J. F. Regan, G. A. Karlin-Neumann, C. M. Hindson, S. Saxonov and B. W. Colston, *Anal. Chem.*, 2011, **83**, 8604–8610.
13 S. Sakakihara, S. Araki, R. Iino and H. Noji, *Lab Chip*, 2010, **10**, 3355–3362.
14 B. Vogelstein and K. W. Kinzler, *Proc. Natl. Acad. Sci. U. S. A.*, 1999, **96**, 9236–9241.
15 E. A. Ottesen, J. W. Hong, S. R. Quake and J. R. Leadbetter, *Science*, 2006, **314**, 1464–1467.
16 D. M. Rissin, C. W. Kan, T. G. Campbell, S. C. Howes, D. R. Fournier, L. Song, T. Piech, P. P. Patel, L. Chang, A. J. Rivnak, E. P. Ferrell, J. D. Randall, G. K. Provuncher, D. R. Walt and D. C. Duffy, *Nat. Biotechnol.*, 2010, **28**, 595–599.
17 C. W. Kan, A. J. Rivnak, T. G. Campbell, T. Piech, D. M. Rissin, M. Mosl, A. Peterca, H. P. Niederberger, K. A. Minnehan, P. P. Patel, E. P. Ferrell, R. E. Meyer, L. Chang, D. H. Wilson, D. R. Fournier and D. C. Duffy, *Lab Chip*, 2012, **12**, 977–985.
18 H. Zhang, S. Nie, C. M. Etson, R. M. Wang and D. R. Walt, *Lab on a chip*, 2012.
19 M. Margulies, M. Egholm, W. E. Altman, S. Attiya, J. S. Bader, L. A. Bemben, J. Berka, M. S. Braverman, Y. J. Chen, Z. Chen, S. B. Dewell, L. Du, J. M. Fierro, X. V. Gomes, B. C. Godwin, W. He, S. Helgesen, C. H. Ho, G. P. Irzyk, S. C. Jando, M. L. Alenquer, T. P. Jarvie, K. B. Jirage, J. B. Kim, J. R. Knight, J. R. Lanza, J. H. Leamon, S. M. Lefkowitz, M. Lei, J. Li, K. L. Lohman, H. Lu, V. B. Makhijani, K. E. McDade, M. P. McKenna, E. W. Myers, E. Nickerson, J. R. Nobile, R. Plant, B. P. Puc, M. T. Ronan, G. T. Roth, G. J. Sarkis, J. F. Simons, J. W. Simpson, M. Srinivasan, K. R. Tartaro, A. Tomasz, K. A. Vogt, G. A. Volkmer, S. H. Wang, Y. Wang, M. P. Weiner, P. Yu, R. F. Begley and J. M. Rothberg, *Nature*, 2005, **437**, 376–380.
20 J. Y. Park, M. Morgan, A. N. Sachs, J. Samorezov, R. Teller, Y. Shen, K. J. Pienta and S. Takayama, *Microfluid. Nanofluid.*, 2010, **8**, 263–268.
21 K. Sasagawa, K. Ando, T. Kobayashi, T. Noda, T. Tokuda, S. H. Kim, R. Iino, H. Noji and J. Ohta, *Jpn. J. Appl. Phys.*, 2012, **51**, 02BL01.